AWARD NUMBER: W81XWH-11-1-0109

TITLE: Novel CXCR3/CXCR7-Directed Biological Antagonist for Inhibition of Breast Cancer Progression

PRINCIPAL INVESTIGATOR: Dr. James Lillard, Jr.

CONTRACTING ORGANIZATION: Morehouse School of Medicine, Inc.
Atlanta, GA 30310-1458

REPORT DATE: November 2013

TYPE OF REPORT: Final

PREPARED FOR: U.S. Army Medical Research and Materiel Command
Fort Detrick, Maryland 21702-5012

REPORT DOCUMENTATION PAGE

Form Approved
OMB No. 0704-0188

1. REPORT DATE *(DD-MM-YYYY)*	2. REPORT TYPE	3. DATES COVERED *(From - To)*
November 2013	Final	01-Sept-2011 to 31-Aug-2013

4. TITLE AND SUBTITLE
Novel CXCR3/CXCR7-Directed Biological Antagonist for Inhibition of Breast Cancer Progression

5a. CONTRACT NUMBER

5b. GRANT NUMBER
W81XWH-11-1-0109

5c. PROGRAM ELEMENT NUMBER

6. AUTHOR(S)

James W. Lillard, Jr.

email: jlillard@msm.edu

5d. PROJECT NUMBER

5e. TASK NUMBER

5f. WORK UNIT NUMBER

7. PERFORMING ORGANIZATION NAME(S) AND ADDRESS(ES)

Morehouse School of Medicine, Inc.
720 Westview Drive S.W.
Atlanta, GA 30310-1495

8. PERFORMING ORGANIZATION REPORT NUMBER

9. SPONSORING / MONITORING AGENCY NAME(S) AND ADDRESS(ES)
U.S. Army Medical Research and Materiel Command
Fort Detrick, Maryland 21702

10. SPONSOR/MONITOR'S ACRONYM(S)

11. SPONSOR/MONITOR'S REPORT NUMBER(S)

12. DISTRIBUTION / AVAILABILITY STATEMENT
Approved for Public Release; Distribution Unlimited

13. SUPPLEMENTARY NOTES

14. ABSTRACT

Docetaxel, a well-established anti-mitotic agent, has been shown in large clinical trials to improve survival and is arguably the standard of care for breast cancer (BrCa) that no longer respond to other therapies. Unfortunately, docetaxel has a number of serious side effects. Therapies that simultaneously prevent BrCa progression and improve docetaxel efficacy are greatly needed. To this end, the numerous anti-apoptotic mechanisms employed by BrCa cells to survive serum-free environments or apoptosis-inducing agents are not entirely known. Chemokines support BrCa progression and cell survival; BrCa cells express CXCR3, CXCR4, and CXCR7, which bind CXCL11 and/or CXCL12. We created a mutant CXCR3/CXCR7 ligand-immunoglobulin fusion protein (mut-CXCL11-Ig) that lacks immunogenic, glycosaminoglycan (GAG)-binding sites but retains the ability to bind, but not activate CXCR3 and CXCR7 receptors. While we had difficulty scaling-up the production of the mut-CXCL11-Ig candidate, we report we have developed a new expression system for production and future animal studies. We also report CXCR3/CXCR4/CXCR7 expression are higher during the G2 phase of BrCa cell cycle, supporting proliferation. CXCL11-Ig reduces chemokine receptor expression, increases docetaxel-driven apoptosis, and reduces CXCL12-dependent cell growth. These studies provide important and new information regarding the cellular and molecular mechanisms, following CXCL11/CXCL12 and CXCR3/CXCR4/CXCR7 interactions, which modulate BrCa progression. Importantly, these studies are the first required to demonstrate the efficacy of mut-CXCL11-Ig for BrCa.

15. SUBJECT TERMS

Nothing Listed

16. SECURITY CLASSIFICATION OF: U			17. LIMITATION OF ABSTRACT	18. NUMBER OF PAGES	19a. NAME OF RESPONSIBLE PERSON
					USAMRMC
a. REPORT	b. ABSTRACT	c. THIS PAGE	UU	25	19b. TELEPHONE NUMBER *(include area code)*
U	U	U			

Standard Form 298 (Rev. 8-98)
Prescribed by ANSI Std. Z39.18

Table of Contents

Page

Introduction……..3

KEYWORDS……4

OVERALL PROJECT SUMMARY…… 5

Key Research Accomplishments……20

Reportable Outcomes……21

Conclusion……20

References……22

INTRODUCTION:

Treatment modalities for breast cancer (BrCa) have improved therapeutic outcomes, but 40% will ultimately die from this disease, highlighting the need for new therapies. Docetaxel is a well-established anti-mitotic chemotherapy that has recently been shown in large clinical trials to improve survival and is arguably the standard of care for BrCa that no longer respond to hormone or Herceptin therapies (i.e., triple negative). However, docetaxel has a number of serious side effects in the majority of patients, due to non-tumor interactions causing nephrotoxicity, neurotoxicity, nausea/vomiting, myelosuppression (thrombocytopenia and neutropenia), hearing loss, and death. Hence, therapies that simultaneously prevent BrCa progression and improve docetaxel efficacy are greatly needed. To this end, the numerous anti-apoptotic mechanisms employed by BrCa cells to survive serum-free environments or apoptosis-inducing agents (e.g., docetaxel) are not entirely known, yet significantly contribute to BrCa's morbidity and mortality. Chemokines have been shown to support BrCa progression and cell survival. BrCa cells express CXCR3, CXCR4, and CXCR7, which if stimulated can support invasion and cell survival. The ligands for CXCR7 are CXCL11, which also binds CXCR3, and CXCL12, which also binds CXCR4. CXCL11 and CXCL12 are expressed by stroma, activated vascular and lymphatic endothelial cells, and tumor associated macrophages that can all support survival or promote invasion of leukocytes (or BrCa cells). Indeed, these CXCR7 ligands are elevated in tissues and serum from patients with a variety of systemic diseases (including BrCa). To solve this problem of $CXCR7^{+}$ BrCa cell stimulation, we created a mutant CXCR3/CXCR7 ligand-immunoglobulin fusion protein (mut-CXCL11-Ig) that lacks immunogenic, glycosaminoglycan (GAG)-binding sites but retains the ability to tightly bind, but not activate CXCR3 and CXCR7 receptors. It is important to note that chemokine receptor signaling following ligand-binding can lead to signaling, which supports cell survival, growth, and/or cell invasion. Previously, we demonstrated our mut-CXCL11-Ig inhibits signaling required for growth and matrix metalloproteinase (MMP) expression by BrCa cells. We also had significantly greater bioavailability (~ 5 days) than compared to native CXCL11 (~30 minutes) or CXCR3 and CXCR7 small molecule antagonists (< 6 hours) without liver toxicity (unlike small molecule inhibitors). These previous studies provided biological and clinical rationales to support the *hypothesis* that *CXCL11 and CXCL12 interactions promote BrCa cell survival and invasion, which can be inhibited with a single biological antagonist - mut-CXCL11-Ig.*

KEYWORDS:
Chemokine
Chemokine receptor
CXCL11
CXCL12
CXCR4
CXCR7
Breast cancer
Triple negative
Docetaxel

OVERALL PROJECT SUMMARY:

Our studies showed **(1)** CXCR7 expression (earlier stages) is significantly higher in advanced BrCa cases than compared to non-neoplastic tissue, which does not express detectable levels of CXCR7; **(2)** CXCR7 and CXCR3 mRNAs are elevated in BrCa cell lines (MCF-7, MDA-MB-231) compared to MCF-10A (normal breast); **(3)** Amnis ImageStream analysis, which allows single cell 40X fluorescent image acquisition and analysis by flow, revealed that CXCL11 stimulates CXCR3 and CXCR7 aggregation and rapid desensitization, CXCL12 modulates modest CXCR7 clustering; mut-CXCL11-Ig abrogates CXCL11 and CXCL12 stimulation of CXCR7; **(4)** Mut-CXCL11-Ig inhibits CXCR7-mediated growth and MMP expression by blocking CXCL11 and CXCL12 stimulation; and **(5)** The nonGAG-binding mut-CXCL11-Ig has a bioavailability of ~1 week without apparent cardiac, liver, pancreatic or renal toxicities. Together, these findings provide the rationale to support the hypothesis that ***CXCL11 and CXCL12 interactions promote BrCa cell survival and invasion, which can be inhibited with a single biological antagonist - mut-CXCL11-Ig.*** Two aims were used to test this hypothesis. ***Aim One*** assessed the use of mut-CXCL11-Ig to impede breast tumor growth and MMP expression. ***Aim Two*** characterized the mechanisms of mut-CXCL11-Ig that modulate BrCa progression in the presence and absence of docetaxel**.** It is important to mention that we encountered **significant obstacles** that delayed completion of the proposed work. First, our move from University of Louisville to Morehouse School of Medicine delayed the start of the project to the Fall of 2011. Secondly, the stable cell line engineered to express wtCXCL11-Ig and mutCXCL11-Ig proteins failed and it took another year to generate new cells to express these proteins. Lastly, the breeding of animals to generate F3 PyMT-Luc ($CXCR3^{+/+}$ or $CXCR3^{-/-}$) mice was not successful. Our approved Statement of Work laid-out the following tasks, which I have summarized as either completed or not completed.

Aim One will assess the use of mut-CXCL11-Ig to impede breast tumor growth and MMP expression.

Task 1.1 (**completed**): Immunogenic residues that also provide CXCL11 the ability to bind GAG were removed to engineer mut-CXCL11-Ig. Mouse anti-mut-CXCL11-Ig humoral and helper T lymphocyte (HTL) responses have been evaluated to confirm that these modifications reduced the immunogenicity of this therapeutic protein.

Task 1.2 and 1.3 (**partially completed**, due to low production levels of CXCL11-Ig proteins and inability to make nonGAG-binding CXCL11-Ig): Unfortunately, the nonGAG-binding CXCL11-Ig was not stable and did not consistently form dimers required for serum stability. Hence, only 10 mg/kg/week of Control-Ig or mut-CXCL11-Ig were used to treat MDA-MB-231-luciferase-positive (luc) as well as MCF-7-luc xenografts. Mammary fat pad of 96 NIH-III mice were used to orthotopically graft MDA-MB-231-luc and MCF-7-luc cell lines. Breast tumor progression were followed non-invasively by *in vivo* imaging. Breast tumors from task 1.2 were excised to quantify levels of caspase-3/9, Ki67, and MMP expression by histology.

Task 1.4, 1.5, and 1.6 (**not completed**): Initially, we aimed to use 10 mg/kg/week of Control-Ig, nonGAG-binding CXCL11-Ig, or mut-CXCL11-Ig to treat novel $CXCR3^{+/+}$ and $CXCR3^{-/-}$ MMTV-PyVT (PyMT)-luc mice that would have presumably developed tumors. However, after several attempts, we were not successful in creating/bredding the PyMT-luc mice.

Aim Two will characterize the mechanisms of mut-CXCL11-Ig that modulate BrCa progression in the presence and absence of docetaxel.

Task 2.1, 2.2, 2.3, 2.4 (**partially completed**, due to low production levels of CXCL11-Ig proteins and inability to make serum stable nonGAG-binding CXCL11-Ig): MDA-MB-231-luc and MCF-7-luc were orthotopically implanted into mammary fat pads of NIH-III mice. After tumor formation, 10^6 photons/sec, mice from task 2.1 were treated with optimal (10 mg/kg/week) or suboptimal (0.1 mg/kg/week) doses of docetaxel and/or 10 mg/kg/week of Control-Ig or mut-CXCL11-Ig. 4T1-luc tumor-bearing wildtype mice were treated with optimal (10 mg/kg/week) or suboptimal (0.1 mg/kg/week) doses of docetaxel and/or 10 mg/kg/week of mut-CXCL11-Ig. Breast tumor progression was non-invasively imaged to monitor growth.

METHODS

Cell Culture: Human BrCa cell lines, MCF-7 (HTB-22) and MDA-MB-231 (HTB-26), were purchased from American Type Cell Culture. Primary human mammary epithelial cells (HMEC) were obtained from LONZA. HMEC, MCF-7, and MDA-MB-231 cell lines were used for all experiments performed and discussed. HMEC were maintained in MEGM supplemented with 2ml of BPE, 2ml of hydrocortisone, 2 ml of human epithelial growth factor (hEGF), 500 l of insulin, and 2 ml of gentamicin/amphotericin-B. MCF-7 and MDA-MB-231 cells were maintained in IMEM and DMEM (Gibco-Invitrogen) media, respectively, supplemented with 10% FBS (Hyclone-Fisher), without phenol red and 5 µg/ml of penicillin/streptomycin (Gibco) at 37°C with 5% CO_2. Cells were cultured for 3 days in complete culture media then lifted with cell-stripper (Gibco) before being counted with trypan blue by the Cellometer^{TM} Auto T4 (Nexcelom Biosciences). Cells were seeded (5 x 10^5 cells per well) in 6-well plates (Corning-Fisher) containing 1% serum and allowed to acclimate overnight before being treated. Treatments included no addition, 100 ng/ml of CXCL12 (SCYB12; R&D Systems), 100 ng/ml of CXCL12 + 100 ng/ml of pertussis toxin (List Biological Laboratories), 100 ng/ml of CXCL12 + 6 µM of U73122 (Sigma). Cells were treated with inhibitors one hour prior to the addition of CXCL12 and allowed to incubate for 16 hours. Media was collected and stored at -80°C and used for ELISA-based assays. Cells were used for total RNA isolation using the TRIzol method.

Cell lines & Animals: MDA-MB-231-luc, MCF-7-luc, and 4T1-luc cell lines were purchased Caliper/Xenogen or Dr. Patrick Casey, respectively. These cell lines rapidly develop tumors when orthotopically injected in mammary fat pad of Nu/Xid mice. Cells from these xenografts metastasize within 6 weeks on implantation; however, mice that receive MCF-7-luc cells were also require subcutaneous implantation of estrogen pellets (17β-Estradiol, 0.36 mg/pellet, 60 day release), which were obtained from Innovative Research of America (Sarasota, FL). Six week old female NIH-bg-nu-Xid mice (NCI-Frederick) received 10^6 of MDA-MB-231-luc or MCF-7-luc cells in 100 µL of saline by orthotopic mammary fat pad injection under anesthesia with pentobarbital (0.05 mg/g body weight).

***Immuno-staining and Morphometric Analysis*:** After tumor excision, frozen sectioning, sections were blocked with 2% goat serum and incubated with FITC-conjugated anti-phospho ERK1/2, AKT, and GSK-3β (BD Pharmingen, R&D Systems, and Santa Cruz Biotechnology), PE-conjugated anti-MMP Abs (R&D Systems and Santa Cruz Biotechnology), and PE-Cy5-conjugated anti-luciferase Abs (Invitrogen). Abs were applied in serial and the slides were developed and counterstained with a dilution of DAPI. Linear regression analysis were used to test the significances of tissue pathology and relevance of phospho ERK1/2, AKT, and GSK-3β as well as MMP expression. Morphometric analysis of sections were performed with the aid of Spectrum Plus software (Aperio Technologies). Automated image analysis will be performed Spectrum Plus algorithms for i) Positive Pixel count and Color Deconvolution; ii) Immunohistochemistry Membrane; iii) Immunohistochemistry Nuclear; and iv) Micromet.

Imagestream analysis of protein expression and localization: PE/Cy5 conjugated anti-human CXCR4 antibody (clone#12G5) was purchased from Biolegend, Inc. Polyclonal rabbit anti-CXCR7 antibody was purchased from GeneTex, Inc and conjugated with a donkey-anti-rabbit-FITC antibody (R&D Systems). BrCa cells were seeded in 6-well non-adherent plates at 10^6 cells/well in media containing 1% FBS and allowed to acclimate 3 hours before treatment. Cells were treated according to the above-mentioned protocols and cell suspensions from each well were taken at 0 and 5 minute time-points and collected for further analysis. Cell suspensions were centrifuged at 200 x g for 10 minutes at 4°C to pellet cells, supernatants were removed and cells were resuspended in 500 µl of paraformaldehyde (PFA) / phosphate buffered saline (PBS) solution for 10 minutes at RT. Again, cells were centrifuged at 200 x g for 10 minutes at 4°C to pellet cells, supernatants were removed and cells were resuspended in 100 µl of saponin solution for 30 minutes at RT. Cell suspensions were centrifuged at 200 x g for 10 minutes at 4°C, supernatants were removed and cells were resuspended in 1 µg (per 10^6 cells) of primary antibody solution, which consisted of PE-Cy5-conjugated anti-mouse CXCR4, FITC-conjugated anti-mouse CXCR7, Alexa Fluor 488-conjugated or PE-conjugated anti-mouse NF-kB p65, PE-conjugated anti-mouse ERK1/2 antibodies and/or 7AAD (BD) for 30 min at room temperature. Next, 1ml of fluorescence-activated cell sorting (FACS) buffer (1% bovine serum albumin (BSA) in PBS) to remove any unbound antibodies. Cell suspensions were centrifuged at 200 x g for 10 minutes at 4°C to pellet cells;

supernatants were removed and cells were resuspended in 100 µl of FACS buffer. Analyses were performed using Amnis ImageStream, which allows for flow cytometry-based image acquisition and analysis with six channel (Bright filed, dark filed, and four channel for different fluorochrome). This flow-based image acquisition device is supported by INSPIRE™ software and statistical results gathered using Amnis IDEAS™ software (Amnis Corporation). To explain, the Amnis ImageStream 100 was the first commercially available imaging flow cytometer. It combines advantages of flow cytometry with those of image analysis (digital imagery of each individual cell, calculation of morphological changes, subcellular localization or co-localization of fluorescent probes). Offering several advantages over flow cytometry analysis or microscopic analysis of fluorescently stained cells.

The images were stored in a compensated image file (CIF) for subsequent analysis using IDEAS software which quantifies change in fluorescent probe pixel intensities in: area of mask in pixels, aspect ratio of mask, weighted aspect ratio of mask, mean intensity of pixels outside of mask, standard deviation of intensity of pixels outside of mask, centroid of mask in horizontal axis, intensity-weighted centroid of mask in horizontal axis, centroid of mask in vertical axis, intensity-weighted centroid of mask in vertical axis, total intensity of image using logical "OR" of all six image masks, variance of intensity of pixels within masks, maximum intensity gradient of pixels within mask, radius mean square (RMS) of intensity gradient of pixels within mask, background-corrected sum of pixel intensities within mask, major axis of mask in pixels, intensity-weighted major axis of mask in pixels, total Intensity of image divided by area of mask, minimum pixel intensity within mask, minor axis of mask in pixels, intensity-weighted minor axis of mask in pixels, angle of major axis relative to axis of flow, angle of intensity-weighted major axis relative to axis of flow, maximum pixel intensity within mask, number of edge pixels in mask, maximum pixel intensity within large bright spots, sum of pixel intensities within large bright spots, maximum pixel intensity within medium-sized bright spots, sum of pixel intensities within medium-sized bright spots, un-normalized maximum pixel intensity within large bright spots, sum of un-normalized pixel intensities within large bright spots, maximum pixel intensity within small bright spots, sum of pixel intensities within small bright spots, sum of pixel intensities within mask, number of spots detected in image, area of logical "OR" of all six image masks in pixels, camera line readout rate in Hertz at time object was imaged, unique object number, pixel intensity correlation between two images of the same object, and user-defined algebraic combination of imagery and masks, user-defined masks using (erode, dilate, threshold, and boolean combinations), and any boolean combination of user-defined populations.

MTT cell proliferation assay: Breast cancer cells, MCF7 and MDA-MB-231, were treated with different concentrations of CXCL11-IgG fusion proteins IL2ss.CXCL11(1-73). hIgG1Fc (wt) and IL2ss.CXCL11(4-73). hIgG1Fc (mt) and proliferation was measured using MTT [3-(4,5-dimethylthiazol-2-yl)-2,5-diphenyltetrazolium bromide] assay. Briefly, cells were seeded in 96-well plates at a density of 10,000 cells per well per 100 µl media and allowed to adhere for 24 h, followed by addition of wt- and mt-CXCL11-IgG proteins at 0, 50, 100, 200, 400 and 800 ng/ml. Plates in triplicates were then incubated for 24, 48, or 72 h. Each day, 3 hours prior to the end of incubation times, the plates were centrifuged at 200 x *g* for 5 minutes to pellet potential floating cells, then media were aspirated out of wells and 100 µl of fresh media containing MTT (5mg/ml) was added to each well. Plates were returned to incubator for an additional 3 h. At the end of incubation time, media was aspirated out of wells, and 200 µl DMSO was added to each well to solubilize the formazan crystals. Plates were then read with a microplate spectrophotometer at 540 nm. The absorbance of formazan dye solution is in direct proportion to the number of proliferating cells per well.

Flow Cytometry Analysis: *CXCR3/CXCR4/CXCR7 expression:* Breast cancer cells, MCF7 and MDA-MB-231, were treated with wt- and mt- CXCL11-IgG fusion proteins (500 ng/ml) for 48h and expression of CXCR- 3, 4, and 7 was analyzed using FACS. CXCL11 (100 ng/ml), CXCL12 (100 ng/ml) treated and untreated cells were used as controls. Fluorescein (FITC)-conjugated mouse anti-human CXCR3, Allophycocyanin (APC)-conjugated mouse anti-human CXCR4 and Phycoerythrin (PE)-conjugated mouse anti-human CXCR7 antibody and their respective isotype controls were purchased from R&D Systems. Breast cancer cells were washed three times in phosphate buffered saline (PBS) [supplemented with 1% bovine serum albumin (BSA)] and treated with 1.0 µg of Fc Block (Pharmingen) per 10^6 cells for 15 min at room temperature. Fc-blocked cells were stained with 1.0 µg of FITC-, APC-, PE- conjugated mouse anti-human CXCR3, CXCR4, CXCR7 antibodies or respective isotype control antibodies per 10^6 cells at 4˚C for 1 h. Subsequently, the cells were washed with 2.0

ml of fluorescence-activated cell-sorting (FACS) buffer (1% BSA in PBS) to remove unbound antibodies. Following washing, 10µl of 7-AAD, a nuclear stain, was added to each tube. Next, labeled cells were fixed in 500 µl of 2% paraformaldehyde solution, and 10^5 cells were analyzed by flow cytometry (FACS ARIA II, BD Biosciences) and data were analyzed using Flow Jo software 8.8.7 for MAC (Tree star Inc., Ashland, OR).

Cell cycle analysis and stage specific expression of CXCR3/CXCR4/CXCR7 in treated and untreated cells: BrCa cells ($1x10^6$) were treated with wt- and mt-CXCL11-IgG fusion proteins (500 ng/ml) for 48h, and cell cycle distribution was determined by 7-AAD staining using BD FACS ARIA II as described previously. CXCL11 (100 ng/ml), CXCL12 (100 ng/ml) treated and untreated cells were used as controls. Data were analyzed using Flow Jo software 8.8.7 for MAC.

Annexin V/7AAD assay for Apoptosis: For apoptosis assay, BrCa cells ($1x10^6$) were treated with wt- and mt-CXCL11-IgG fusion proteins (500 ng/ml), CXCL12 (100 ng/ml), and Gemcitabine (6 µM) for 48h, stained with annexin V-FITC and 7-AAD, according to the manufacturer's protocol (Biolegend, San Diego, CA) and evaluated by BD FACS ARIA II. Untreated cells, and cells treated only with gemcitabine were used as controls. CXCL12 was used as growth factor in all the wells. Data were analyzed using Flow Jo software 8.8.7 for MAC.

RESULTS

Table 1. CXCR7, CXCR4, and CXCR3 antagonist bioavailabilities and toxicities.

			Toxicities		
Antagonist	Affinity	Serum Half-Life	Liver	Cardiac	Reference
CCX451/CCX754	5 nM, CXCR7	< 6 hours	+	-	(Burns et al.) (WO/2005/074645)
AMD3100	12 nM, CXCR4	< 6 hours	+/-	+	(Allen et al.)
AMG487	7 nM, CXCR3	< 6 hours	+	-	(Heise et al.; Wijtmans et al.)
CXCL11	1.4 nM, CXCR3 5 nM, CXCR7	< 12 hours	-	-	(Burns et al.; Cole et al.)
mut-CXCL11-Ig	10 nM, CXCR3 7.5 nM, CXCR7	5 days	-	-	US Patent #8,541,564 US Patent #8,796,422

**Radio-ligand binding was quantified by analyzing $CXCR3^+$ and $CXCR7^+$ cells in a γ counter (Perkin-Elmer). Data were analyzed and plotted using software (Prism; GraphPad).*

Expression of CXCR7 by Breast Tumors: Prior studies in our laboratory and others have shown chemokine receptor expression by various carcinomas (Singh et al., 2004a; Singh et al., 2004b). We confirmed *in vivo* protein expression of CXCR7 by breast tumor tissue. Immunohistochemistry was performed using deparaffinized TMAs stained with DAB (brown), which is representative of CXCR7, and counterstained with hematoxylin **(Figure 3)**. CXCR7 expression was elevated in breast tumors staged asT1 (n = 10), T2 (n = 40), T3 (n = 15), and T4 (n = 4) and compared with non-neoplastic breast tissue from the same subject (i.e., n = 69). CXCR7 expression was significantly higher in all breast tumor tissue than compared to benign tissue and highest in T4 > T1, T2, and T3 staged tumor tissue. While expression of CXCR7 in breast tumors did not correlate with stage, a trend of cytoplasmic to nucleur localization of CXCR7 expression was observed when comparing early stage with advanced stage cases, respectively. Amnis ImageStream confirmed strong CXCR7 and CXCR4 protein, cell-surface expression by MCF-7 and MDA-MB-231 cell lines **(Figures 4)**. Cell density plots, which analyzed both positive and negative events of each receptor, show the percentage of cells that were positive either for CXCR7, CXCR4, or both receptors. The percent distribution displayed in each cell density plot was based on the intensity of each receptor's protein expression. These findings demonstrate that CXCR4 and CXCR7 protein expression does not precisely correlate with mRNA expression in these cell lines. Further, these results suggest post-transcriptional and/or -translational modification of chemokine receptors may occur, which would not doubt effect their function.

Receptor expression during the cell cycle as well as translocation was also determined using untreated BrCa cells. MCF-7 and MDA-MB-231 cell lines showed high expression of both CXCR7 and CXCR4 in G_2 phase of the cell cycle, with moderate to low expression for S and comparatively low expression during G_0/G1

phases **(Figure 5)**. HMECs showed a similar pattern. Interestingly, this pattern of chemokine receptor expression supports the notion that chemokine receptor signaling during the cell cycle might promote cell survival and proliferation. It is important to mention that while CXCR4 expression is largely confined to the cytoplasm during BrCa progression, the expression of CXCR7 is localized to tumor cell nuclei for advanced BrCa cases. When comparing BrCa cell lines and HMECs**,** CXCR4 and CXCR7 translocated to the nucleus of cells after CXCL12 stimulation **(Figures 6 and 7)**.

CXCL12 is a powerful chemo-attractant that stimulates bi-directional migration, invasion, and survival of breast cancer cells (Huang et al., 2007). I examined whether the interactions of CXCL12-CXCR4/7 are involved in signal-transduction pathways that lead to these events. Previous studies have shown that phosphorylation of ERK1/2 in lung cancer cells is involved in cell migration and invasion (Fernandis et al., 2004). Other studies have shown that NFκB activation is necessary for cell migration and invasion of other cancer cells (Boukerche et al., 2007). To determine if ERK1/2 and NFκB are activated by CXCR4/CXCR7 by CXCL12, *in vitro* assays followed by Amnis ImageStream analysis were performed. Untreated HMECs and BrCa cell lines expressed moderate to high protein levels of phosphorylated ERK1/2 and NFκB in the cytosol **(Figures 8)**. After CXCL12 stimulation, both phosphorylated NFκB and ERK1/2 translocated to the nuclei of BrCa cell lines **(Figures 9)**. This demonstrates that detection of CXCL12 by CXCR4 and/or CXCR7 transduces cell signals leading to the activation of both ERK1/2 and NF-kB and their translocation to the nucleus.

IL2ss.CXCL11.hIgG4Fc sequence

```
                                                    ~~~~~~~
                                                                                IL-2 secretion signal
                                                                             MetTyrArg MetGlnLeu LeuSerCysIle
501      TCTGTTCTGC GCCGTTACAG ATCCAAGCTG TGACCGGCGC CTACCTGAGA TCACCGGCGA AGGAGGCCA CCATGTACAG GATGCAACTC CTGTCTTGCA
                                  EcoRI
                                  ~~~~~~~          CXCL11 (1-73)
         ·IAlaLeuSer LeuAlaLeu ValThrAsnSer PheProMet PheLysArg GlyArgCysLeu CysIleGly ProGlyVal LysAlaValLys ValAlaAsp·
601      TTGCACTAAG TCTTGCACTT GTCACGAATT CGTTCCCCAT GTTCAAAAGA GGACGCTGTC TTTGCATAGC CCCTGGGTA AAAGCAGTAA AAGTGGCAGA
         ·IleGluLys AlaSerIleMet TyrProSer AsnAsnCys AspLysIleGlu ValIleIle ThrLeuLys GluAsnLysGly GlnArgCys LeuAsnPro
701      TATTGAAAAA GCCTCCATAA TGTACCCAAC TAACAACTGT GACAAAATAG AAGTGATTAT TACCCTGAAA GAAAATAAAG GACAACGATG CCTAAATCCC
                                                                                  human IgG4 Fc (constant region)
         LysSerLysGln AlaArgLeu IleIleLys LysValGluArg LysAsnPhe ProProCys ProSerCysPro AlaProGlu PheLeuGly GlyProSerVal
801      AAATCTAAGC AACGAAGCT TATAATCAAA AAAGTTGAAA GAAAGAATTT TCCCCCATGC CCATCATGCC CAGCACCTGA GTTCCTGGGG GGACCATCAG
         ·VPheLeuPhe ProProLys ProLysAspThr LeuMetIle SerArgThr ProGluValThr CysValVal ValAspVal SerGlnGluAsp ProGluVal·
901      TCTTCCTGTT CCCCCCAAAA CCCAAGGACA CTCTCATGAT CTCCCGGACC CCTGAGGTCA CGTGCGTGGT GTGGACGTG AGCCAGGAAG ACCCCGAGGT
         ·GlnPheAsn TrpTyrValAsp GlyValGlu ValHisAsn AlaLysThrLys ProArgGlu GluGlnPhe AsnSerThrTyr ArgValVal SerValLeu
1001     CCAGTTCAAC TGGTACGTGG ATGGCGTGGA GGTGCATAAT GCCAAGACAA AGCCGCGGGA GGAGCAGTTC AACAGCACGT ACCGTGTGGT CAGCGTCCTC
         ThrValLeuHis GlnAspTrp LeuAsnGly LysGluTyrLys CysLysVal SerAsnLys GlyLeuProSer SerIleGlu LysThrIle SerLysAlaLys
1101     ACCGTCCTGC ACCAGGACTG GCTGAACGGC AAGGAGTACA AGTGCAAGGT CTCCAACAAA GCCCTCCCGT CCTCCATCGA GAAAACCATC TCCAAAGCCA
         ·LGlyGlnPro ArgGluPro GlnValTyrThr LeuProPro SerGlnGlu GluMetThrLys AsnGlnVal SerLeuThr CysLeuValLys GlyPheTyr·
1201     AAGGGCAGCC CCGAGAGCCA CAGGTGTACA CCCTGCCCCC ATCCCAGGAG GAGATGACCA AGAACCAGGT CAGCCTGACC TGCCTGGTCA AAGGCTTCTA
         ·ProSerAsp IleAlaValGlu TrpGluSer AsnGlyGln ProGluAsnAsn TyrLysThr ThrProPro ValLeuAspSer AspGlySer PheLeuLeu
1301     CCCCAGCGAC ATCGCCGTGG AGTGGGAGAG CAATGGGCAG CCGGAGAACA ACTACAAGAC CACGCCTCCC GTGCTGGACT CCGACGGCTC CTTCTTCCTC
         TyrSerArgLeu ThrValAsp LysSerArg TrpGlnGluGly AsnValPhe SerCysSer ValMetHisGlu AlaLeuHis AsnHisTyr ThrGlnLysSer
1401     TACAGCAGGC TAACCGTGGA CAAGAGCAGG TGGCAGGAGG GGAATGTCTT CTCATGCTCC GTGATGCATG AGGCTCTGCA CAACCACTAC ACACAGAAGA
                                        BamI
                                        NheI
         ·SLeuSerLeu SerProGly Lys***
1501     GCCTCTCCCT GTCTCCGGGT AAATGAGTGC TAGCTGGCCA GACATGATAA GATACATTGA TGAGTTTGGA CAAACCACAA CTAGAATGCA GTGAAAAAAA
```

IL2ss.CXCL11(4-73).hIgG1Fc sequence

```
                                                    ~~~~~~~
                                                                                IL-2 secretion signal
                                                                             MetTyrArg MetGlnLeu LeuSerCysIle
501      TCTGTTCTGC GCCGTTACAG ATCCAAGCTG TGACCGGCGC CTACCTGAGA TCACCGGCGA AGGAGGCCA CCATGTACAG GATGCAACTC CTGTCTTGCA
                                  EcoRI
                                  ~~~~~~~   CXCL11 (4-73)
         ·IAlaLeuSer LeuAlaLeu ValThrAsnSer PheLysArg GlyArgCys LeuCysIleGly ProGlyVal LysAlaVal LysValAlaAsp IleGluLys·
601      TTGCACTAAG TCTTGCACTT GTCACGAATT CGTTCAAAAG AGGACGCTGT CTTTGCATAG CCCCTGGGT AAAAGCAGTG AAAGTGGCAG ATATTGAAAA
         ·AlaSerIle MetTyrProSer AsnAsnCys AspLysIle GluValIleIle ThrLeuLys GluAsnLys GlyGlnArgCys LeuAsnPro LysSerLys
701      AGCCTCCATA ATGTACCCAA CTAACAACTG TGACAAAATA GAAGTGATTA TTACCCTGAA AGAAAATAAA GGACAACGAT GCCTAAATCC CAAATCAAAG
                                                                                  human IgG1 Fc (constant region)
         GlnAlaArgLeu IleIleLys LysValGlu ArgLysAsnPhe AspLysThr HisThrCys ProProCysPro AlaProGlu LeuLeuGly GlyProSerVal
801      CAAGCAAGGC TTATAATCAA AAAAGTTGAA AGAAAGAATT TTGACAAAAC TCACACATGC CCACCGTGCC CAGCACCTGA ACTCCTGGGG GGACCGTCAG
         ·VPheLeuPhe ProProLys ProLysAspThr LeuMetIle SerArgThr ProGluValThr CysValVal ValAspVal SerHisGluAsp ProGluVal·
901      TCTTCCTCTT CCCCCCAAAA CCCAAGGACA CCCTCATGAT CTCCCGGACC CCTGAGGTCA CATGCGTGGT GTGGACGTG AGCCACGAAG ACCCTGAGGT
         ·LysPheAsn TrpTyrValAsp GlyValGlu ValHisAsn AlaLysThrLys ProArgGlu GluGlnTyr AsnSerThrTyr ArgValVal SerValLeu
1001     CAAGTTCAAC TGGTACGTGG ACGGCGTGGA GGTGCATAAT GCCAAGACAA AGCCGCGGGA GGAGCAGTAC AACAGCACGT ACCGTGTGGT CAGCGTCCTC
         ThrValLeuHis GlnAspTrp LeuAsnGly LysGluTyrLys CysLysVal SerAsnLys AlaLeuProAla ProIleGlu LysThrIle SerLysAlaLys
1101     ACCGTCCTGC ACCAGGACTG GCTGAATGGC AAGGAGTACA AGTGCAAGGT CTCCAACAAA GCCCTCCCAG CCCCCATCGA GAAAACCATC TCCAAAGCCA
         ·LGlyGlnPro ArgGluPro GlnValTyrThr LeuProPro SerArgGlu GluMetThrLys AsnGlnVal SerLeuThr CysLeuValLys GlyPheTyr·
1201     AAGGGCAGCC CCGAGAACCA CAGGTGTACA CCCTGCCCCC ATCCCGGGAG GAGATGACCA AGAACCAGGT CAGCCTGACC TGCCTGGTCA AAGGCTTCTA
         ·ProSerAsp IleAlaValGlu TrpGluSer AsnGlyGln ProGluAsnAsn TyrLysThr ThrProPro ValLeuAspSer AspGlySer PheLeuLeu
1301     TCCCAGCGAC ATCGCCGTGG AGTGGGAGAG CAATGGGCAG CCGGAGAACA ACTACAAGAC CACGCCTCCC GTGCTGGACT CCGACGGCTC CTTCTTCCTC
         TyrSerLysLeu ThrValAsp LysSerArg TrpGlnGlnGly AsnValPhe SerCysSer ValMetHisGlu AlaLeuHis AsnHisTyr ThrGlnLysSer
1401     TACAGCAAGC TCACCGTGGA CAAGAGCAGG TGGCAGCAGG GGAACGTCTT CTCATGCTCC GTGATGCACG AGGCTCTGCA CAACCACTAC ACGCAGAAGA
                                        BamI
                                        NheI
         ·SLeuSerLeu SerProGly Lys***
1501     GCCTCTCCCT GTCTCCGGGT AAATGAGTGC TAGCTGGCCA GACATGATAA GATACATTGA TGAGTTTGGA CAAACCACAA CTAGAATGCA GTGAAAAAAA
```

Preparation of chemokine-immunoglobulin fusion proteins: Specific chemokine-Ig fusion polypeptides used in this study include wild-type or mutations are named accordingly to indicate the particular mutation. For example, "mut-" before the CXCL11 (e.g., mut-CXCL11) is indicative of an engineered mutation to CXCL11. Specifically, a truncation of the first three N-terminal amino acids of the mature CXCL11 protein. Further, GAG-binding sites were generated by a chemokine-immunoglobulin fusion polypeptide including in the mutant chemokine polypeptide that has been truncated at the N-terminus to remove residues 1-4 and also mutated to substitute alanines (A) for lysines (K) and histidines (H) within neutral amino acids. Finally, this study we use either human wtCXCL11 or (human-derived) mutCXCL11 fused to Fc constant region of IgG subclass 4 Ig. Subsequently, recombinant vectors comprising nucleic acid molecules that encode the polypeptides disclosed were created and expressed in Chinese hamster ovary (CHO) cells to express the desired protein. An unexpected result was that expression of these constructs were not stable in CHO cells. Moreover, the GAG-less CXCL11-Ig constructs did not form stable dimers to optimally antagonize CXCR3 and CXCR7 as well as CXCR4/CXCR7 heterodimers. After incurring these problems and several failed attempts, we redesigned the expression vectors and cell lines to a HEK-239 expression system that produced grams per liter of constructs (**Figure 10**). The SDS-PAGE gel analysis

confirmed the ~38kDa and ~70kDa size of CXCL11-IgG1Fc under reducing and non-reducing conditions, respectively. Importantly, the GAGless CXCL11-IgG1Fc constructs were expressed, but did not form heterodimers.

CXCL11-IgG1Fc fusion proteins inhibit proliferative of BrCa cells: Both wt- and mt-CXCL11-IgG1Fc fusion proteins inhibited the growth of MCF7 and MDA-MB-231 cells in a dose- and time-dependent manner. The anti-proliferative affect on both cell lines was highest at 72 hours after either wt- and mut-CXCL11-IgG1Fc's. However, the response was significantly higher with wt (GAG) proteins, than compared to mut(GAGless)-proteins. The maximum growth inhibition in MCF-7 and MDA-MB-231 cells was found to be ~51% and ~79%, respectively, with wt-CXCL11-IgG1Fc. However, mut-CXCL11-IgG1Fc induced the greatest growth inhibition in MCF-7 and MDA-MB-231 cell lines at 40% and 73%, respectively **(Figure 11)**.

CXCL11-IgG1Fc fusion proteins bind and decrease expression of CXCR3, CXCR4, and CXCR7 by MCF-7 and MDA-MB-231 cells: To determine the binding of CXCL11-IgG1Fc's to CXCR3, CXCR4, and CXCR7, we incubated BrCa cells with wt- or mut- proteins for 48h and analyzed the surface expression of these chemokine receptors by flow cytometry. Untreated, CXCL11-treated and CXCL12-treated cells were used as positive controls to access receptor expression. The expression of receptors (CXCR3/4/7) were significantly decreased following wt-CXCL11-IgG1Fc or mut-CXCL11-IgG1Fc treatment, than compared to controls **(Figure 12)**. The decrease in expression suggests either i) CXCL11-IgG1Fc's bind to CXCR3, CXCR4, and CXCR7 and prevent receptor internalization and subsequent recycling or ii) CXCL11-IgG1Fc's interactions lead to a significant reduction in CXCR3, CXCR4, and CXCR7.

CXCL11-IgG1Fc fusion proteins induce G2/M phase arrest in BrCa cells: We also investigated the influence of cell cycle stage specific expression of CXCL11, CXCL12, and CXCL11-IgG1Fc's. All conditions shifted and arrested BrCa cells at G2 phase (from G1) (**Figure 13, Table 2**). wtCXCL11-IgG1 showed the maximum effect on both MCF7 and MDA-MB-231 cell cycle. We also noted that CXCR3, CXCR4, and CXCR7 expression were highest in G2 phase with little or no expression in S and G1 phases of cell cycle (**Figure 14**). CXCL11-IgG1Fc's were further shown to significantly shift or increase the number of cells in G2 phase in both MCF7 and MDA-MB-231 cells, compared to other culture conditions.

CXCL11-IgG1Fc acts as an adjuvant for docetaxel treatment of triple negative breast cancer cells: Finally, we evaluated the efficacy CXCL11-IgG1Fc alone or as an adjuvant to docetaxel treatment of MDA-MB-231-luc cells. wtCXCL11-IgG1Fc significantly enhanced the efficacy of docetaxel treatment of xenografts (**Figure 15**).

Table 2. Effect of CXC11, CXCL12, and CXCL11-IgG1Fc fusion proteins on cell cycle distribution in MCF-7 and MDA-MB-231 cells.

Treatment		%G1	%S	%G2/M
Untreated	MCF-7	75.9	7.96	20.4
	MDA-MB-231	87.6	4.13	9.37
wt-CXCL11-IgG	MCF-7	4.18	12.7	**99.5***
	MDA-MB-231	26.5	11.2	**70.4***
mt-CXCL11-IgG	MCF-7	10.9	21	**76.8***
	MDA-MB-231	23	21.1	**64.6***
CXCL11	MCF-7	0.066	13.3	**85.8***
	MDA-MB-231	17.9	9.64	**71.1***
CXCL12	MCF-7	0	9.77	**97.6***
	MDA-MB-231	14.4	5.95	**79.1***

**BrCa cells were treated with wt- or mt-CXCL11-IgG1Fc (500 ng/mL) for 48 hours, stained with 7AAD, cell cycle distribution was acquired by flow cytometry, and data were analyzed analyzed using FlowJo V.10.*

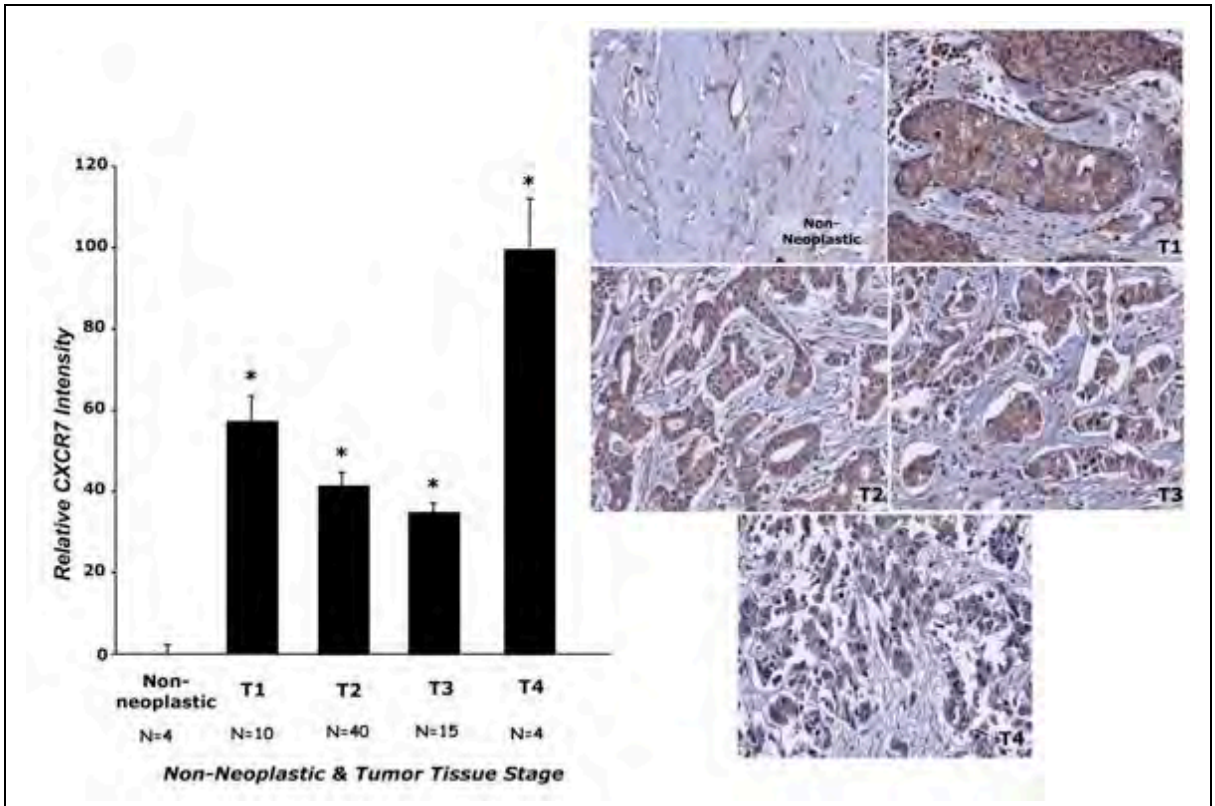

Figure 3. Relative CXCR7 Expression by non-neoplastic and malignant breast tissues. Previously evaluated samples were stained for CXCR7. Relative expression (i.e., colorimetric intensity) ± SD by non-neoplastic (n = 4) breast tissue and T1 (n = 10), T2 (n = 40), T3 (n = 15), and T4 (n = 2) staged tumors are shown in the left panel. Representative CXCR7 (DAB-brown) and hemotoxylin-counter-stained (20X magnification) sections are shown in the right panels.

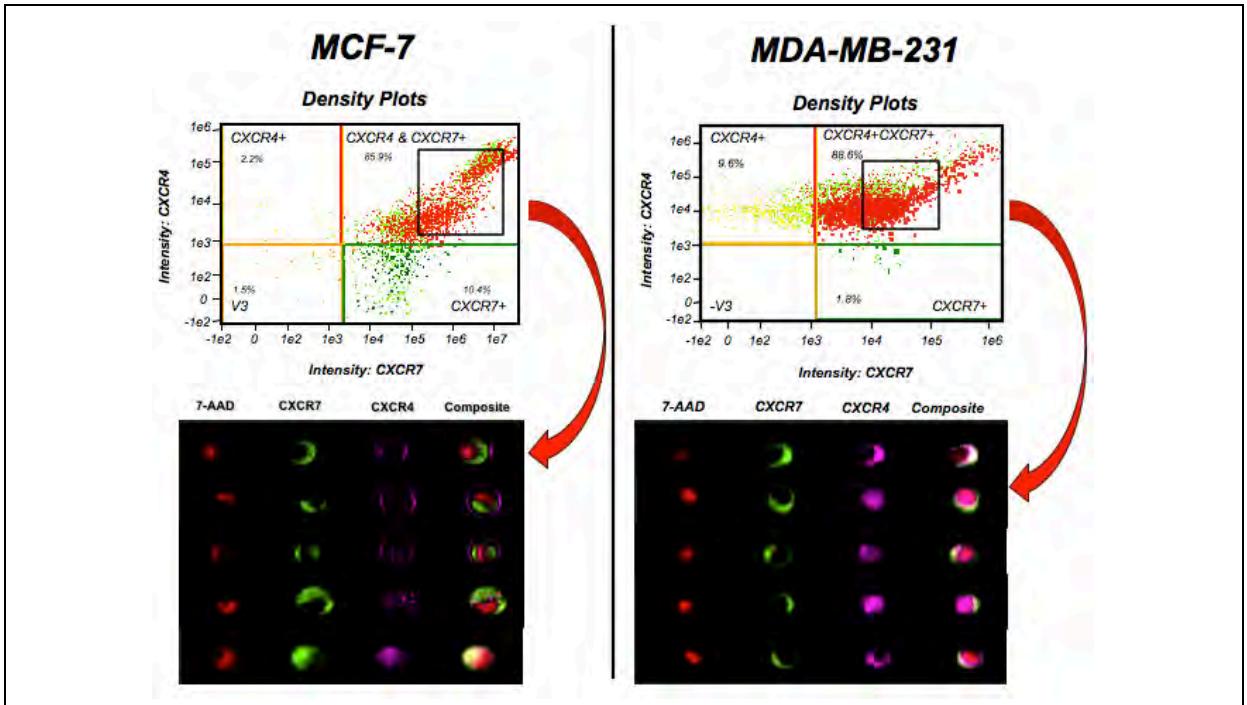

Figure 4. Protein expression and cellular distribution of CXCR4 and CXCR7 by BrCa cell lines. MCF-7 and MDA-MB-231 cells were stained with polyclonal-rabbit anti-CXCR7 antibody conjugated with donkey-anti-rabbit-FITC and PE/Cy5 anti-human CXCR4 antibody. After staining, cells were washed with FACS buffer and analyzed. 7-AAD was used to stain the nucleus and quantified using Amnis Imagestream System. Image analyses were performed using Image Data Exploration Analysis Software (IDEAS). Top panels show density plots of cell populations. Bottom panels from left to right is 7-AAD (red), CXCR7 (green), CXCR4 (purple), and composite respectively.

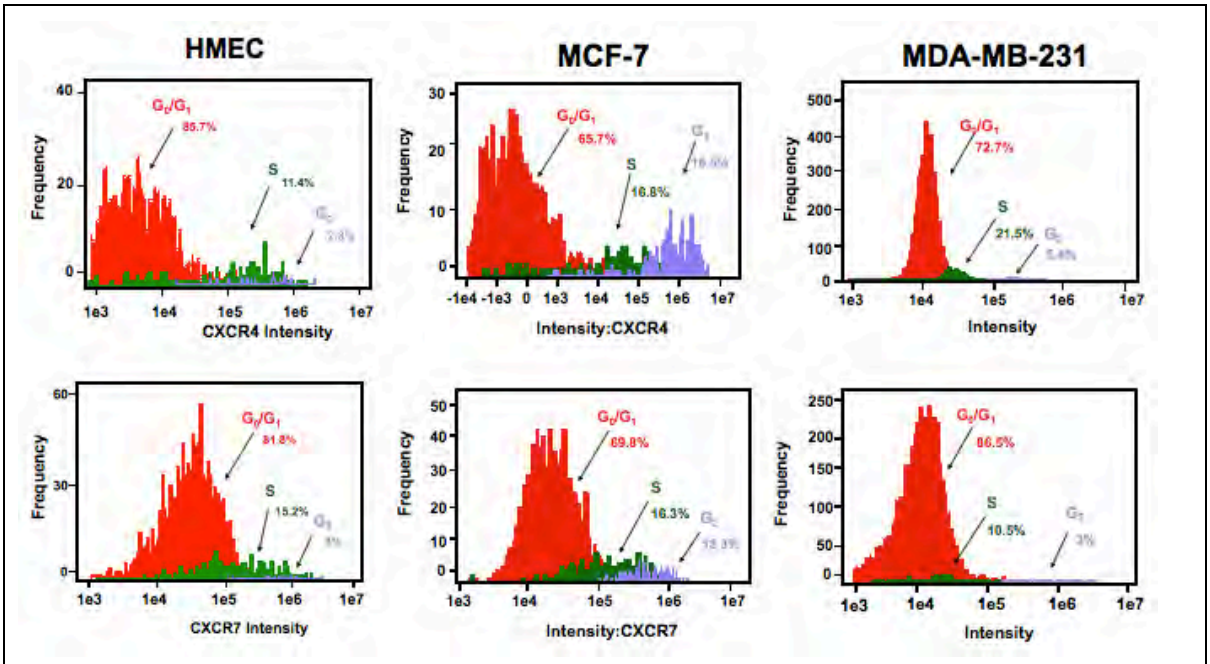

Figure 5. Cell cycle-dependent CXCR4 and CXCR7 expression by (untreated) primary mammary and BrCa cell lines. HMEC cells as well as MCF-7 and MDA-MB-231 cell lines were stained with polyclonal-rabbit anti-CXCR7 antibody conjugated with donkey-anti-rabbit-FITC and PE/Cy5 anti-human CXCR4 antibody and 7AAD was used to stain cell nuclei. After staining, cells were quantified by Amnis ImageStream and analyzed using Amnis IDEAS. Histograms represent cell populations CXCR4 and CXCR7 intensity.

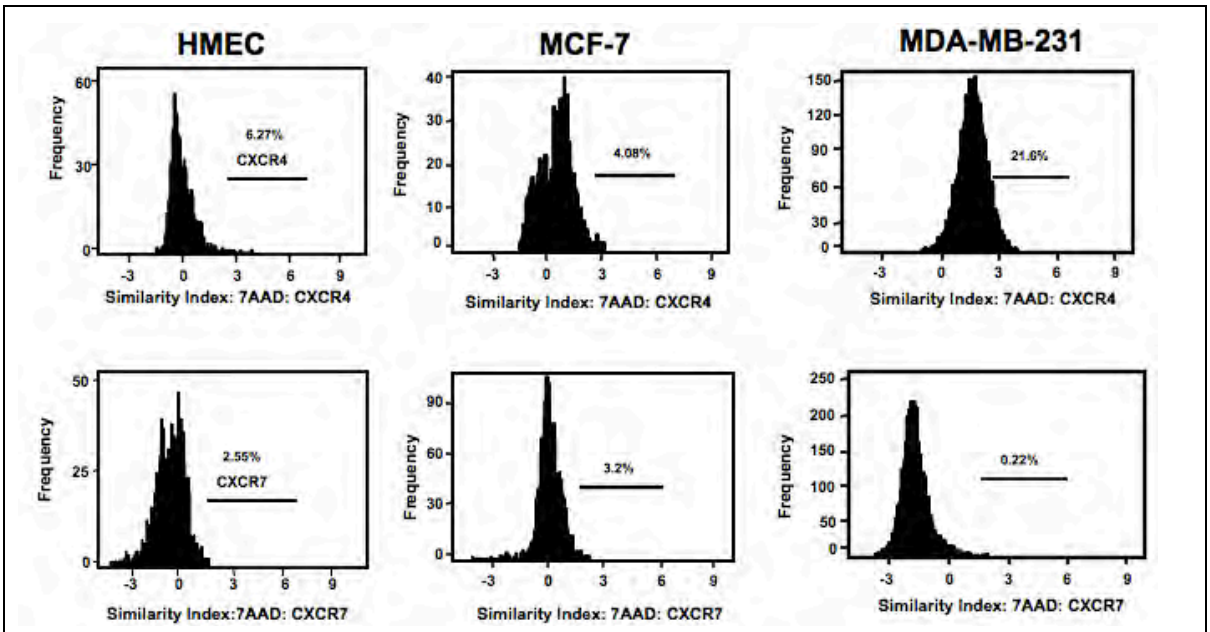

Figure 6. Expression and intracelluar distribution of CXCR4 and CXCR7 in (untreated) primary mammary and BrCa cells. HMEC, MCF-7 and MDA-MB-231 cell lines were stained with polyclonal-rabbit anti-CXCR7 antibody, FITC-conjugated donkey-anti-rabbit antibody, and PE/Cy5-conjugated anti-human CXCR4 antibody and 7AAD was used to stain cell nuclei. After staining, cells were quantified by Amnis ImageStream and analyzed using Amnis IDEAS. Histograms represent cell populations CXCR4 and CXCR7 intensity. Panels show the spatial ratio of CXCR4 or CXCR7 and their nuclei intensities as a histograms.

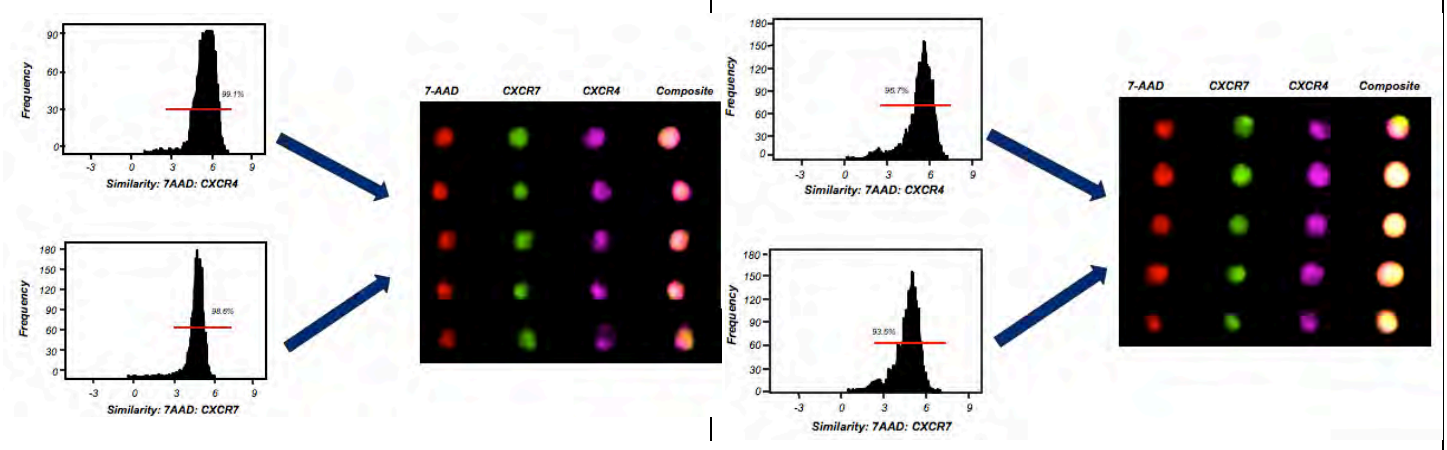

Figure 7. CXCR4 and CXCR7 cytoplasmic to nucleus translocation and expression by MDA-MB-231 and MCF-7 cell lines. MCF-7 cells were treated with 100 ng/ml of CXCL12 for 5 minutes and stained with polyclonal-rabbit anti-CXCR7 antibody, FITC-conjugated donkey-anti-rabbit antibody, PE/Cy5-conjugated anti-human CXCR4 antibody, and 7AAD to stain cell nuclei. After staining, cells were quantified by Amnis ImageStream and images analyzed using Amnis IDEAS. The spatial ratio of CXCR4/CXCR7 and nuclei intensities are shown as histograms representing chemokine receptor nuclear localization or translocation. The right panel shows representative images of the major cell population.

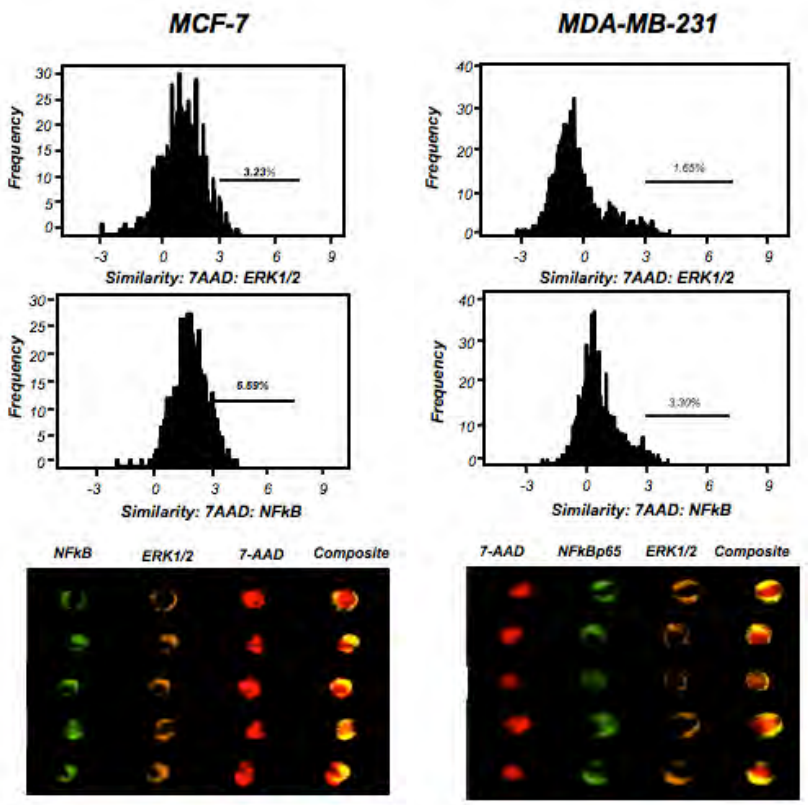

Figure 8. NFκB and ERK1/2 activation state and cellular distribution by resting (untreated) BrCa cells. MCF-7 and MDA-MD-231 cell lines were stained with Alexa Fluor 488-conjugated mouse anti-NFκB p65 and PE-conjugated mouse anti-ERK1/2 antibodies. 7-AAD was used to stain the nucleus. Subsequently, images of cells were acquired by Amnis ImageStream and analyzed using IDEAS software. The top panels show the spatial ratio of NFκB, ERK1/2, and nuclei intensities and co-localization as a histogram. The bottom panel shows representative 7-AAD (red), NFκB (green), ERK1/2 (orange), and composite images of the major cell populations.

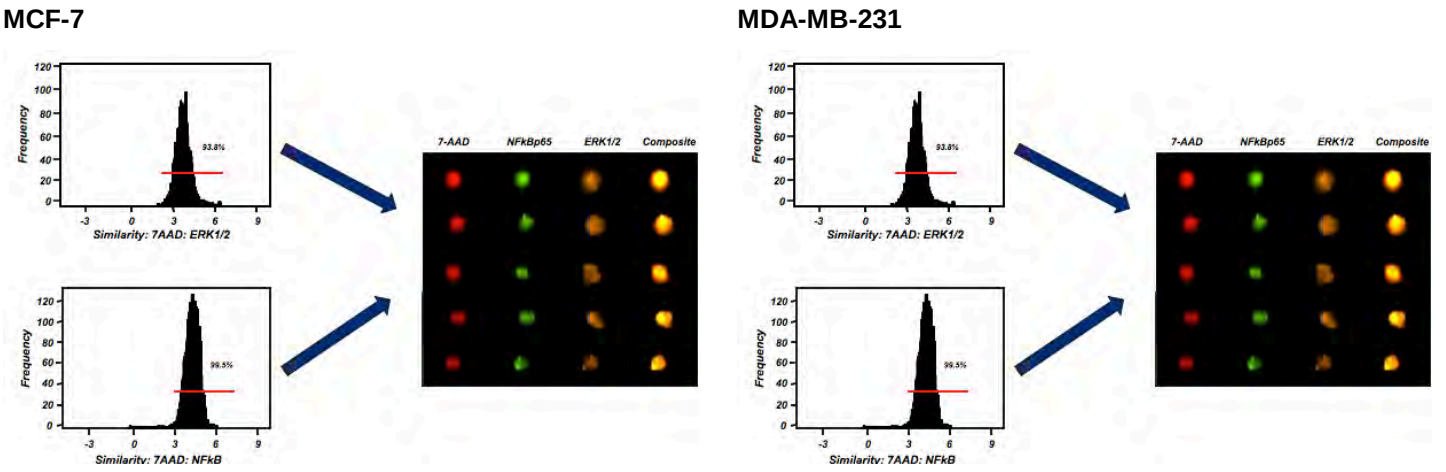

Figure 9. NFκB and ERK1/2 expression and cytoplasmic to nuclear translocation by CXCL12-treated MCF-7 cells. MCF-7 and MDA-MB-231 cells were stained with Alexa Fluor 488-conjugated mouse anti-NFκB p65 and PE-conjugated mouse anti-ERK1/2 antibodies. 7-AAD was used to stain the nucleus. Subsequently, images of cells were acquired by Amnis ImageStream and analyzed using IDEAS software. The top panels show the spatial ratio of NFκB, ERK1/2, and nuclei intensities and co-localization as a histogram. The bottom panel shows representative 7-AAD (red), NFκB (green), ERK1/2 (orange), and composite images of the major cell populations.

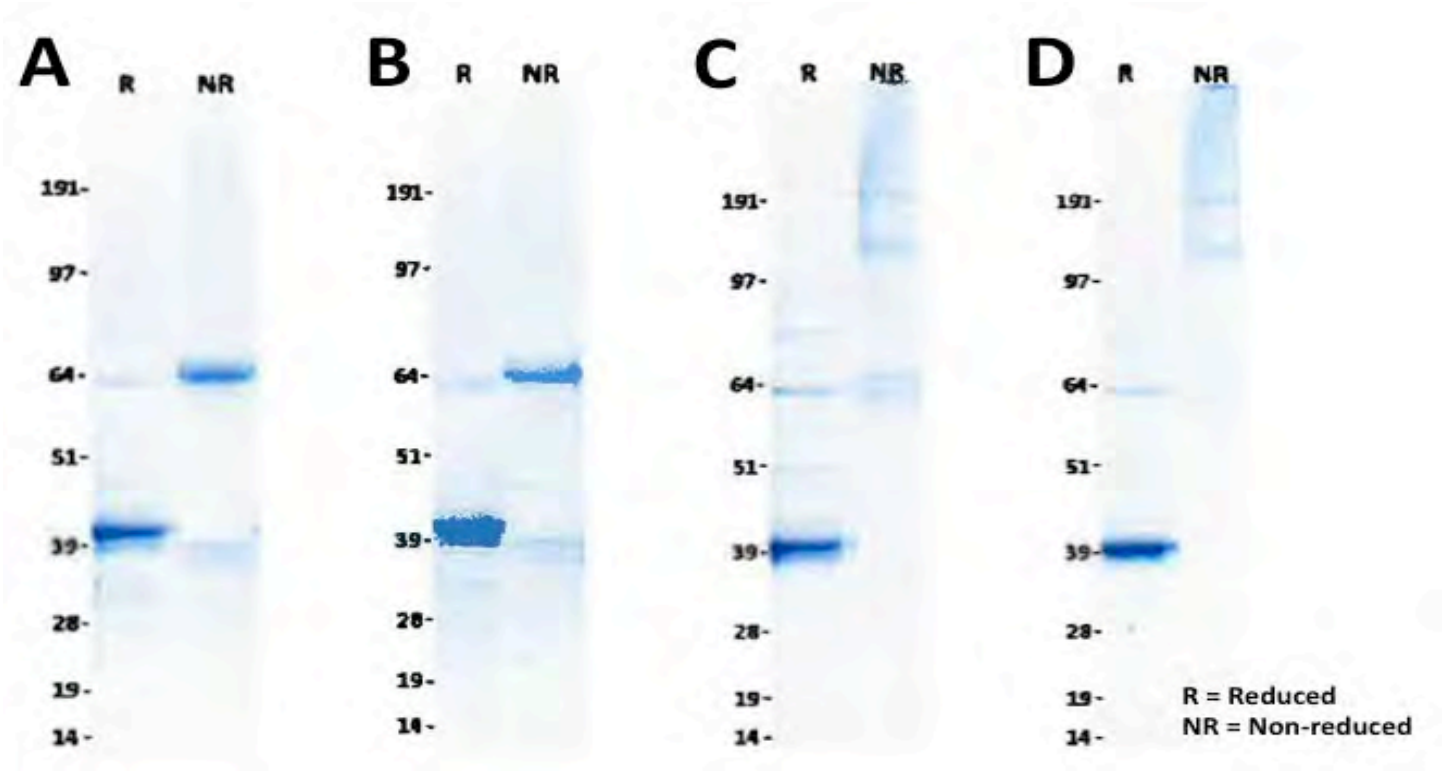

Figure 10. SDS PAGE analysis of HEK-239 cell line expressed CXCL11-IgG1Fc constructs. wtCXCL11-IgG1Fc (A), mutCXCL11-IgG1Fc (B), wtCXCL11-GAGless-IgG1Fc (C), and mutCXCL11-GAGless-IgG1Fc (D) were expressed using human HEK 239 cells. Secreted proteins were captured from serum cell growth medium using protein A columns. Purified proteins were analyzed by NuPAGE Novex Bis-Tris 4-12% gel in both reducing (R) and non-reducing (NR) conditions.

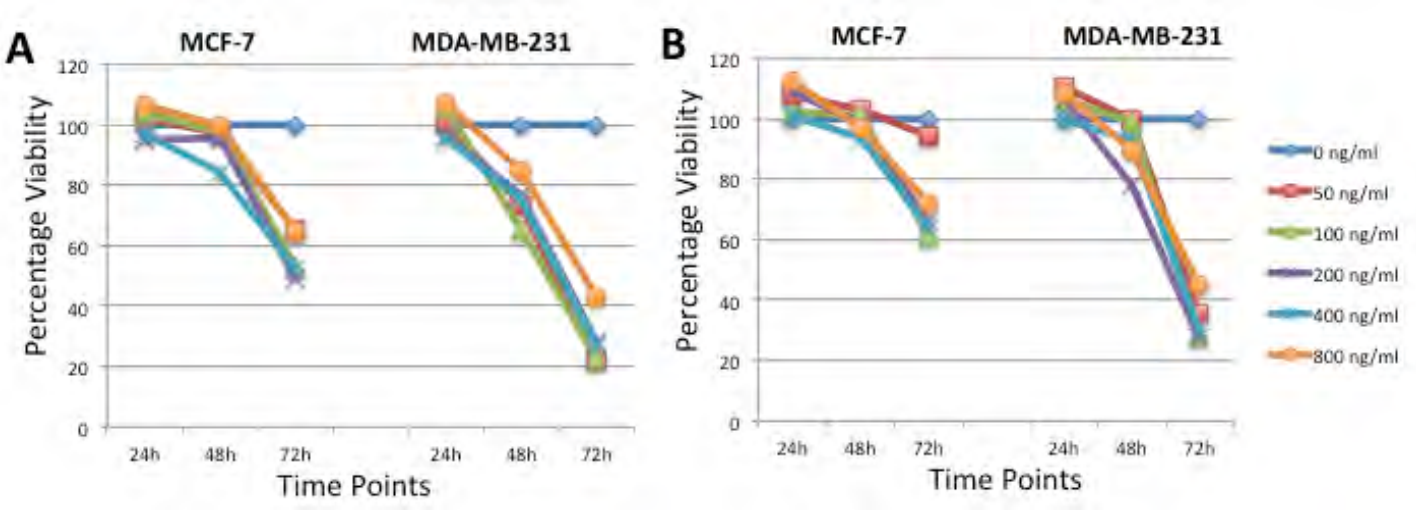

Figure 11. Effect of CXCL11-FcIgG fusion proteins on MCF-7 and MDA-MB-231 cell growth and viability. The effects of MCF-7 and MDA-MB-231 cell viability 24, 48 and 72 hours after wtCXCL11(1-73)-IgG1Fc (Panel A) and mutCXCL11(4-73)-IgIgG1Fc (Panel B) treatment was measured using a MTT assay. The percent of cell viability was calculated as the percentage of the number of treated cells divided by the number of viable cells before treatment.

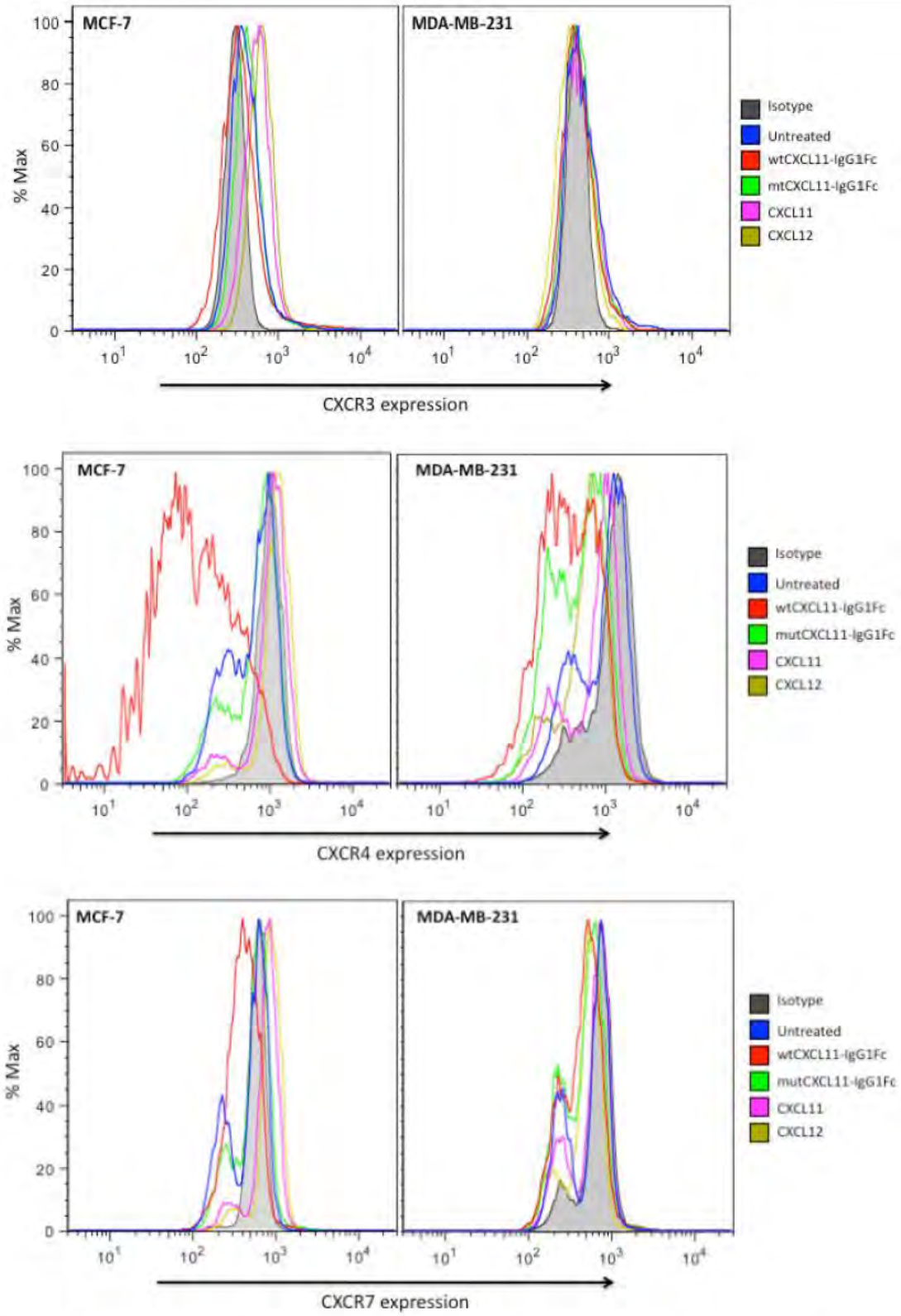

Figure 12. CXCL11, CXCL12, wtCXCL11-IgG1Fc and wtCXCL11-IgG1Fc effects on CXCR3, CXCR4, and CXCR7 expression by MCF-7 and MDA-MB-231 cells. Cells were treated with wtCXCL11-IgG, mtCXCL11-IgG, CXCL11 or CXCL12. After 48 hours, cells were stained with FITC- or PE-conjugated anti-CXCR3, -CXCR4, or –CXCR7 antibodies or respective isotype controls. Next, fluorescent events were acquired using a BD FACS ARIA II and data were analyzed using FlowJo V.10. Flow cytometry analysis showing change in expression of chemokine receptors were represented as either shaded (isotype controls) or solid line (stained) histograms.

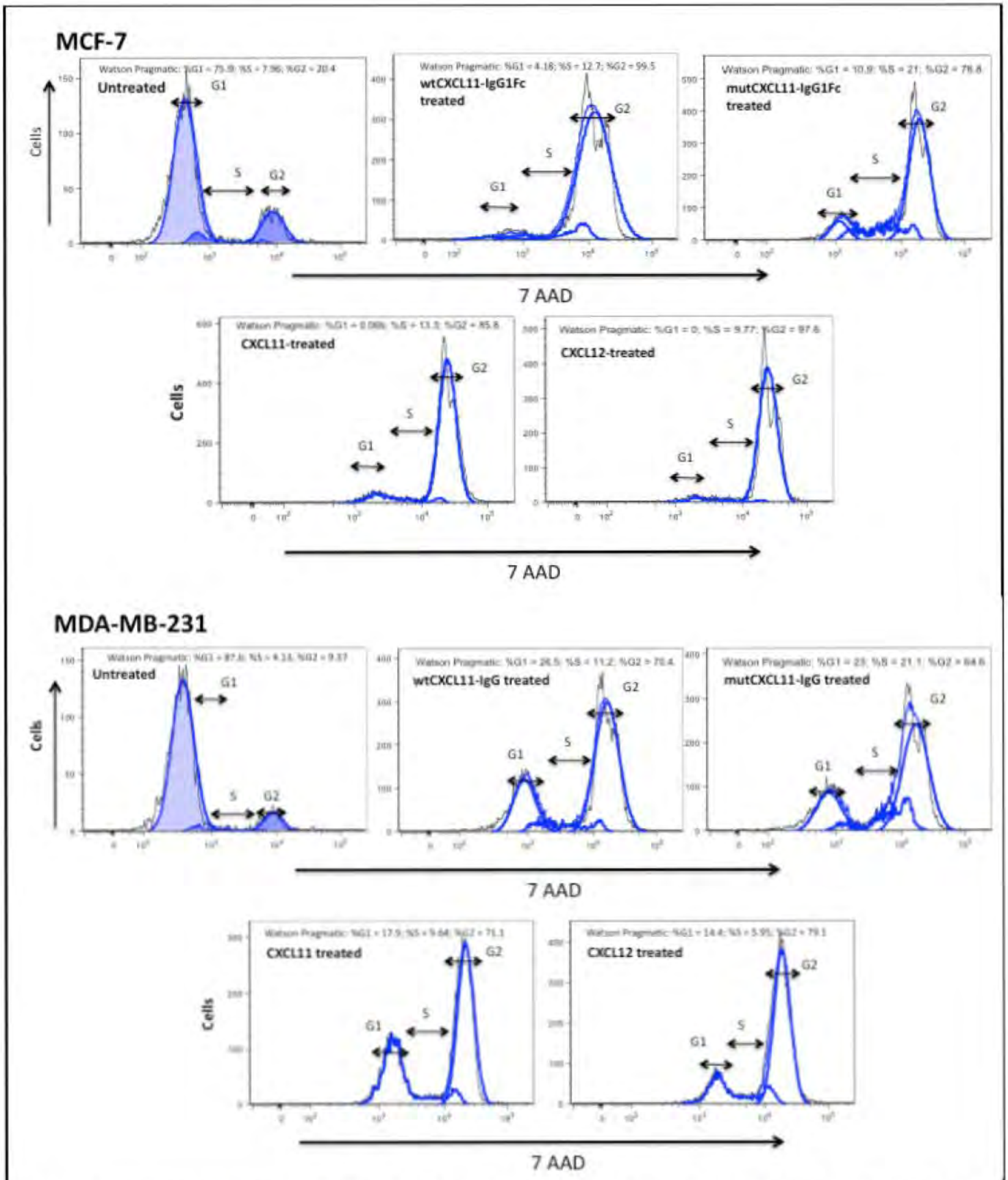

Figure 13. CXCL11, CXCL12, wtCXCL11-IgG1Fc and wtCXCL11-IgG1Fc effects on MCF-7 and MDA-MB-231 cell cycle. Cells were treated with or without wtCXCL11-IgG, mtCXCL11-IgG, CXCL11 or CXCL12. After 48 hours, cells were stained with 7AAD. Next, fluorescent events were acquired using a BD FACS ARIA II and data were analyzed using FlowJo V.10. Flow cytometry analysis showing change in 7AAD uptake by cell nuclei were represented Watson Pragmatic histograms to denote G1, S, and G2 phases of the cell cycle.

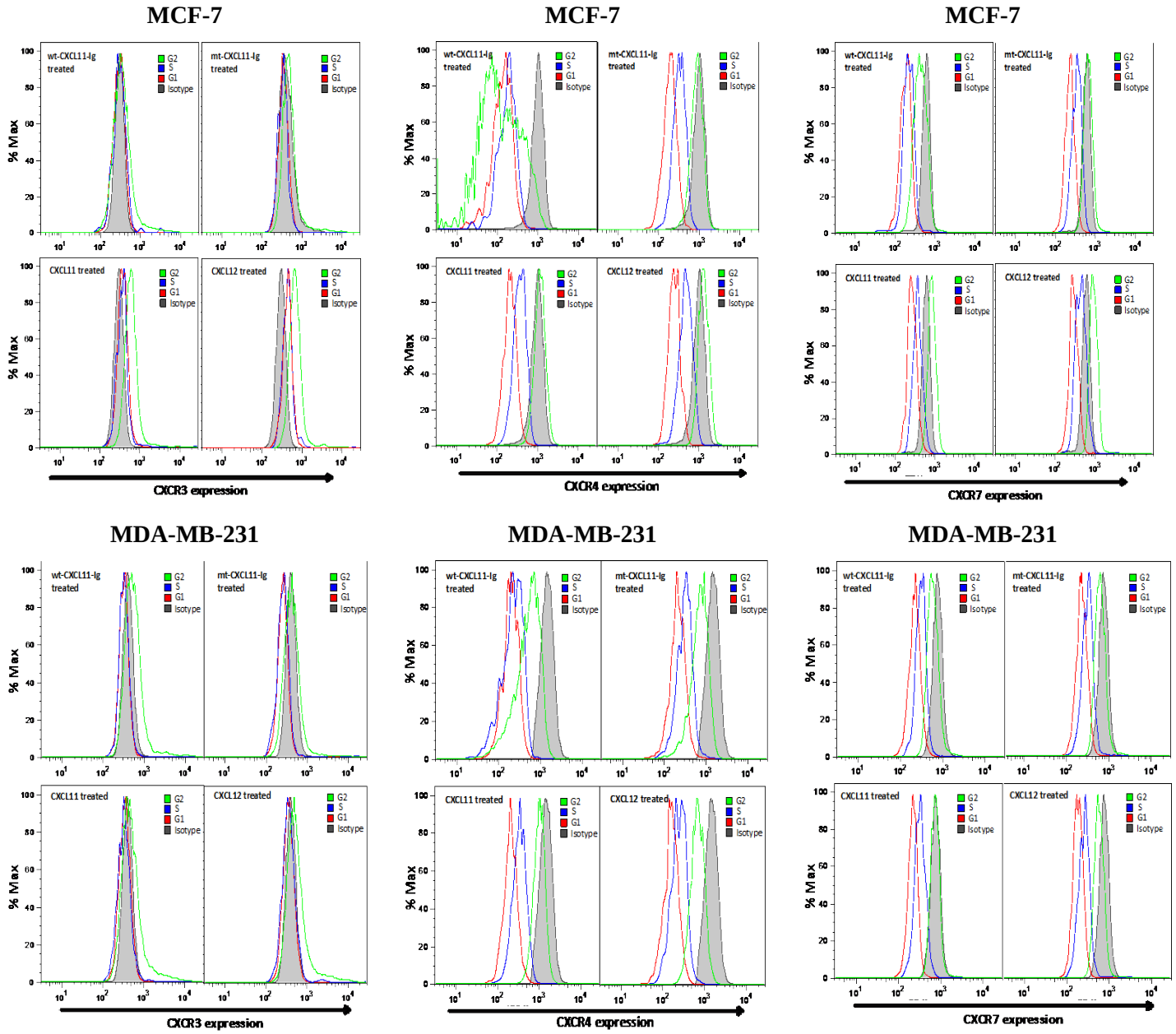

Figure 14. CXCL11, CXCL12, wtCXCL11-IgG1Fc and wtCXCL11-IgG1Fc effects on MCF-7 and MDA-MB-231 cell cycle-dependent CXCR3, CXCR4, and CXCR7 expression. Cells were treated with or without wtCXCL11-IgG, mtCXCL11-IgG, CXCL11 or CXCL12. After 48 hours, cells were stained with FITC- or PE-conjugated anti-CXCR3, -CXCR4, or -CXCR7 antibodies or respective isotype controls. Next, fluorescent events were acquired using a BD FACS ARIA II and data were analyzed using FlowJo V.10. Flow cytometry analysis showing change in expression of chemokine receptors were represented as either shaded (isotype controls) or solid line (stained) histograms. Flow cytometry analysis showing change in 7AAD uptake by cell nuclei were represented Watson Pragmatic histograms to denote G1, S, and G2 phases of the cell cycle.

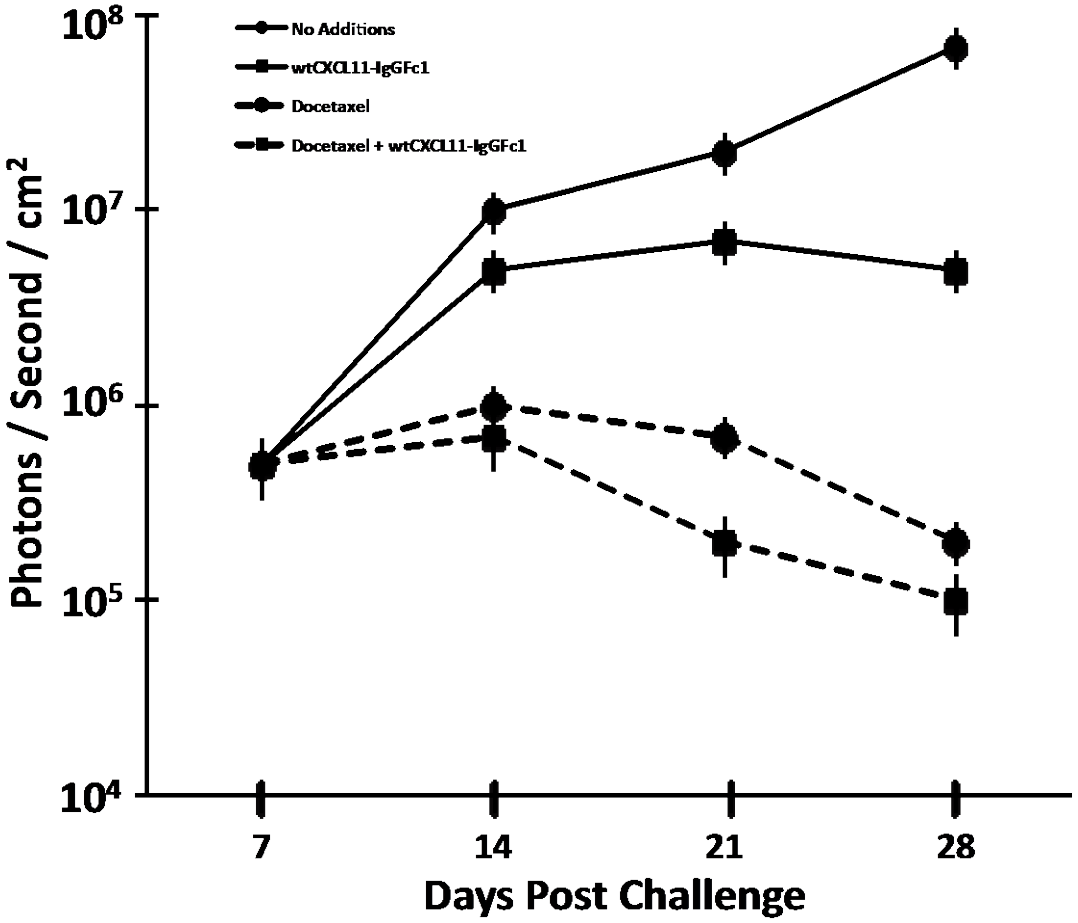

Figure 15. CXCL11-IgG1Fc-mediated tumor regression in MDA-231-luc xenografts. MDA-MB-231-luc cells (10^6) cells were suspended in 100 µL of sterile saline and injected into breast fad pads of nude mice (n =5). After tumors developed to a size of ~100 mm^3, mice were intravenously administered 100 µL of saline alone or 50µg of wtCXCL11-IgG1Fc, 50µg of wtCXCL11-IgG1Fc, 10 mg/kg of docetaxel, or 50µg of wtCXCL11-IgG1Fc plus 10 mg/kg of docetaxel in 100 µL of saline.

KEY RESEARCH ACCOMPLISHMENTS:

- CXCR7 expression was elevated in breast tumors staged asT1 (n = 10), T2 (n = 40), T3 (n = 15), and T4 (n = 4) and compared with non-neoplastic breast tissue from the same subject (i.e., n = 69).
- While expression of CXCR7 in breast tumors did not correlate with stage, a trend of cytoplasmic to nucleur localization of CXCR7 expression was observed when comparing early stage with advanced stage cases, respectively.
- CXCR4 expression is largely confined to the cytoplasm during BrCa progression, the expression of CXCR7 is localized to tumor cell nuclei for advanced BrCa cases.
- These findings demonstrate that CXCR4 and CXCR7 protein expression does not precisely correlate with mRNA expression in these cell lines.
- Receptor expression during the cell cycle as well as translocation was also determined using untreated BrCa cells. MCF-7 and MDA-MB-231 cell lines showed high expression of both CXCR7 and CXCR4 in G_2 phase of the cell cycle, with moderate to low expression for S and comparatively low expression during G_0/G1 phases.
- Detection of CXCL12 by CXCR4 and/or CXCR7 transduces cell signals leading to the activation of both ERK1/2 and NF-kB and their translocation to BrCa cell nuclei.
- CXCL11-IgG1Fc's are ~38kDa and ~70kDa in size of under reducing and non-reducing conditions, respectively. Importantly, the GAGless CXCL11-IgG1Fc construct did not form heterodimers.
- wt-CXCL11-IgG1Fc and mut-CXCL11-IgG1Fc inhibit growth of MCF-7 and MDA-MB-231 cells.
- CXCR3, CXCR4, and CXCR7 were significantly decreased following wt-CXCL11-IgG1Fc or mut-CXCL11-IgG1Fc treatment, than compared to controls.
- CXCL11, CXCL12, and CXCL11-IgG1Fc's shift and/or arrest BrCa cells from G1 to G2 phase.
- CXCL11-IgG1Fc enhanced the efficacy of docetaxel treatment in breast tumor regression, using MDA-MB-231 xenografts.

CONCLUSIONS:

CXCR3 blockade has been shown to reduced lung metastases, but not tumor growth (51). CXCR7 blockade reduces growth of primary tumors and lung metastases as well as impedes cell survival and adhesion (33, 52). While we could not treat mice with GAGless mutant of CXCL11-Ig, our data show CXCL11-IgG1Fc decreased the growth of triple negative breast cancer xenografts. CXCL11-IgG1Fc alone also abrogated breast cancer tumor progression. In future studies we expect that the optimal therapeutic doses of docetaxel can be reduced using CXCL11-IgG1Fc as an adjuvant. The reduction of tumor growth was most likely due to the inhibition of CXCR3-ligands or CXCL12-mediated cell signaling events (i.e., ERK1/2, AKT, GSK, etc.) whereby cells remained in G2 cell cycle phase being more susceptible to docetaxel treatment.

PUBLICATIONS, ABSTRACTS, AND PRESENTATIONS:

Mechanisms Mediated by CXCL12 Signaling through CXCR4 and CXCR7 in Breast Cancer. *American Association for Cancer Research, 101th Annual Meeting.* April 17-21, 2010, Washington, DC.

INVENTIONS, PATENTS AND LICENSES:

Patent Application Serial #: 13/480,526 *(Utility)* Granted Patent: US 8,541,564
Filing Date: 5/25/2012 *(United States)* Date Issued: 9/24/2013

This invention relates to novel chemokine-immunoglobulin fusion polypeptides and uses to treat chemokine receptor-mediated disorders, including cancer and inflammatory disorders.

Patent Application Serial #: 13/962,110 *(Continuation)* Granted Patent: US 8,796,422
Filing Date: 5/25/2012 *(United States)* Date Issued: 8/5/2014

This invention is directed to chemokine-immunoglobulin fusion polypeptides and chemokine-polymer conjugates. The fusion polypeptides and conjugates can be used for treating chemokine receptor-mediated disorders and modulating inflammation, inflammatory cell motility, cancer cell motility, or cancer cell survival.

Application Serial #: 13/962,401 *(Continuation)*
Filing Date: 8/8/2013 *(United States)*

This invention is directed to chemokine-immunoglobulin fusion polypeptides and chemokine-polymer conjugates. The fusion polypeptides and conjugates can be used for treating chemokine receptor-mediated disorders and modulating inflammation, inflammatory cell motility, cancer cell motility, or cancer cell survival.

REPORTABLE OUTCOMES:

There have been no products that have resulted from this research.

REFERENCES:

Docetaxel Allan, L., Morrice, N., Brady, S., Magee, G., Pathak, S., and Clarke, P. (2003). Inhibition of Caspase-9 through Phosphorylation at Thr 125 by ERK-MAPK. Nat Cell Biol *5*, 647-654.

Allen, S. J., Crown, S. E., and Handel, T. M. (2007). Chemokine: receptor structure, interactions, and antagonism. Annu Rev Immunol *25*, 787-820.

Balabanian, K., Lagane, B., Infantino, S., Chow, K. Y. C., Harriague, J., Moepps, B., Arenzana-Seisdedos, F., Thelen, M., and Bachelerie, F. (2005). The chemokine SDF-1/CXCL12 binds to and signals through the orphan receptor RDC1 in T lymphocytes. Journal of Biological Chemistry *280*, 35760-35766.

Balsara, B. R., Apostolou, S., Jhanwar, S. C., and Testa, J. R. (2001). AKT plays a central role in tumorigenesis. Proceeding of National Academy Science of United States of America *98*, 10031-10033.

Biggs, W. H., 3rd, Meisenhelder, J., Hunter, T., Cavenee, W. K., and Arden, K. C. (1999). Protein kinase B/Akt-mediated phosphorylation promotes nuclear exclusion of the winged helix transcription factor FKHR1. Proc Natl Acad Sci U S A *96*, 7421-7426.

Bonaccorsi, L., Marchiani, S., Muratori, M., Carloni, V., Forti, G., and Baldi, E. (2004). Singaling mechanisms that mediates invasion in prostate cancer cells. Annals of the New York Academy of Sciences *1028*, 4693.

Borner, M. M., Myers, C. E., Sartor, O., Sei, Y., Toko, T., Trepel, J. B., and Schneider, E. (1995). Drug-induced apoptosis is not necessarily dependent on macromolecular synthesis or proliferation in the p53-negative human prostate cancer cell line PC-3. Cancer Res *55*, 2122-2128.

Boukerche, H., Su, Z., Emdad, L., Sarkar, D., and Fisher, P. (2007). Mda-9/Syntenin Regulates the Metastatic Phenotype in Human Melanoma Cells By Activating Nuclear Factor-kappa B. Cancer Res *67*, 1812-1822.

Braga, V. (2000). The crossroads between cell-cell adhesion and motility. Nature Cell Biology *2*, E182-184.

Burns, J. M., Summers, B. C., Wang, Y., Melikian, A., Berahovich, R., Miao, Z., Penfold, M. E. T., Sunshine, M. J., Littman, D. R., Kuo, C. J.*, et al.* (2006). A novel chemokine receptor for SDF-1 and I-TAC involved in cell survival, cell adhesion, and tumor development. J Exp Med *203*, 2201-2213.

Cantrell, D. A. (2001). Phosphoinositide 3-kinase signalling pathways. Journal of Cell Science *114*, 1439-1445.

Cole, K. E., Strick, C. A., Paradis, T. J., Ogborne, K. T., Loetscher, M., Gladue, R. P., Lin, W., Boyd, J. G., Moser, B., Wood, D. E.*, et al.* (1998). Interferon-inducible T cell alpha chemoattractant (I-TAC): a novel non-ELR CXC chemokine with potent activity on activated T cells through selective high affinity binding to CXCR3. J Exp Med *187*, 2009-2021.

Datta, S. R., Brunet, A., and Greenberg, M. E. (1999). Cellular survival: a play in three Akts. Genes & Development *13*, 2905-2927.

Denmeade, S. R., and Isaacs, J. T. (1996). Activation of programmed (apoptotic) cell death for the treatment of prostate cancer. Advances in Pharmacology *35*, 281-306.

Dustin, M. L., Bivona, T. G., and Philips, M. R. (2004). Membranes as messengers in T cell adhesion signaling. *Nature Immunology 5*, *363*.

Etienne-Manneville, S., and Hall, A. (2002). Rho GTPases in cell biology. Nature *420*, 629-635.

Fashena, S. J., and Thomas, S. M. (2000). Signalling by adhesion receptors. Nature Cell Biology *2*, E225-229.

Fernandis, A., Prasad, A., Band, H., Klosel, R., and Ganju, R. (2004). Regulation of CXCR4-Mediated Chemotaxis and Chemoinvasion of Breast Cancer Cells. Oncogene *23*, 157-167.

Giagulli, C., Scarpini, E., Ottoboni, L., Narumiya, S., Butcher, E. C., Constantin, G., and Laudanna, C. (2004). RhoA and zeta PKC control distinct modalities of LFA-1 activation by chemokines: critical role of LFA-1 affinity triggering in lymphocyte in vivo homing. Immunity *20*, 25.

Heise, C. E., Pahuja, A., Hudson, S. C., Mistry, M. S., Putnam, A. L., Gross, M. M., Gottlieb, P. A., Wade, W. S., Kiankarimi, M., Schwarz, D.*, et al.* (2005). Pharmacological characterization of CXC chemokine receptor 3 ligands and a small molecule antagonist. J Pharmacol Exp Ther *313*, 1263-1271.

Hendrix, M., Seftor, E., Seftor, R., Kasemeier-Kulesa, J., Kulesa, P., and Postovit, L. (2007). Reprogramming Metastatic Tumour Cells with Embryonic Microenvironments. Nat Rev Cancer *7*, 246-255.

Huang, Y.-C., Hsiao, Y.-C., Chen, Y.-J., Wei, Y.-Y., Lai, T.-H., and Tang, C.-H. (2007). Stromal Cell-Derived Factor-1 Enhances Motility and Integrin Up-regulation Through CXCR4, ERK and NF-kB-Dependent Pathway in Hunman Lung Cancer Cells. Biochemical Pharmacology *74*, 1702-1712.

Ilic, D., Furuta, Y., Kanazawa, S., Takeda, N., Sobue, K., Nakatsuji, N., Nomura, S., Fujimoto, J., Okada, M., and Yamamoto, T. (1995). Reduced cell motility and enhanced focal adhesion contact formation in cells from FAK-deficient mice. Nature *377*, 539-544.

Karin, M. (2006). Nuclear Factor -kB in Cancer Development and Progression. Nature *441*, 431-436.

Kerr, J. F., Wyllie, A. H., and Currie, A. R. (1972). Apoptosis: a basic biological phenomenon with wide-ranging implications in tissue kinetics. British Journal of Cancer *26*, 239-257.

Kyriakis, J. (2000). MAP Kinases and the Regulation of Nuclear Receptors. Science *48*, PE1.

Laudanna, C., Kim, J. Y., Constantin, G., and Butcher, E. (2002). Rapid leukocyte integrin activation by chemokines. Immunological Reviews *186*, 37-46.

Lee, B. C., Lee, T. H., Avraham, S., and Avraham, H. K. (2004). Involvement of the chemokine receptor CXCR4 and its ligand stromal cell-derived factor 1alpha in breast cancer cell migration through human brain microvascular endothelial cells. Molecular Cancer Research: MCR *2*, 327-338.

Liotta, L. A., and Kohn, E. C. (1995). Angiogenesis: role of calcium-mediated signal transduction. Cancer Res *55*, 1856-1862.

Masiero, L., Lapidos, K. A., Ambudkar, I., and Kohn, E. C. (1999). Regulation of the RhoA pathway in human endothelial cell spreading on type IV collagen: role of calcium influx. Journal of Cell Science *112*, 3205-3213.

Miyamoto, S., Teramoto, H., Gutkind, J. S., and Yamada, K. M. (1996). Integrins can collaborate with growth factors for phosphorylation of receptor tyrosine kinases and MAP kinase activation: roles of integrin aggregation and occupancy of receptors. Journal of Cell Biology *135*, 1633-1642.

Nishio, M., Endo, T., Tsukada, N., Ohata, J., Kitada, S., Reed, J., Zvaifler, N., and Kipps, T. (2005). Nurselike cells Express BAFF and APRIL, Which Can Promote Survival of Chronic Lymphocytic Leukemia Cells via a Paracine Pathway Distinct from That of SDF-1 Alpha. Blood *106*, 1824-1830.

Nombela-Arrieta, C., Lacalle, R. A., Montoya, M. C., Kunisaki, Y., Megias, D., Marques, M., Carrera, A. C., Manes, S., Fukui, Y., Martinez, A. C., and Stein, J. V. (2004). Differential requirements for DOCK2 and phosphoinositide-3-kinase gamma during T and B lymphocyte homing. Immunity *21*, 429-441.

Schuler, M., Li, W., Eggers-Sedlet, B., Lee, W., Tailor, P., Fitzgerald, P., Mills, G. B., and Green, D. R. (2001). Linking molecular therapeutics to molecular diagnostics: inhibition of the FRAP/RAFT/TOR component of the PI3K pathway preferentially blocks PTEN mutant cells in vitro and in vivo.[comment]. Journal of Biological Chemistry *276*, 34244-34251.

Shulby, S. A., Dolloff, N. G., Stearns, M. E., Meucci, O., and Fatatis, A. (2004). CX3CR1-fractalkine expression regulates cellular mechanisms involved in adhesion, migration, and survival of human prostate cancer cells. Cancer Res *64*, 4693-4698.

Singh, S., Singh, U. P., Grizzle, W. E., and Lillard, J. W. (2004a). CXCL12-CXCR4 interactions modulates prostate cancer cell migration, metalloproteinase expression and invasion. Laboratory Investigation *84*, 1666-1676.

Singh, S., Singh, U. P., Stiles, J. K., Grizzle, W. E., and Lillard, J. W. (2004b). Expression and Functional Role of CCR9 in Prostate Cancer Cell Migration and Invasion. Clin Cancer Res *10*, 8743-8750.

Wijtmans, M., Verzijl, D., Leurs, R., de Esch, I. J. P., and Smit, M. J. (2008). Towards small-molecule CXCR3 ligands with clinical potential. ChemMedChem *3*, 861-872.

Xue, L., Murray, J. H., and Tolkovsky, A. M. (2000). The Ras/phosphatidylinositol 3-kinase and Ras/ERK pathways function as independent survival modules each of which inhibits a distinct apoptotic signaling pathway in sympathetic neurons. Journal of Biological Chemistry *275*, 8817-8824.

Ye, R. (2001). Regulation of Nuclear Factor -kB Activation by G-Protein Coupled Receptors. J Leukocyte Biol *70*, 839-848.